

Combined use of ion backscattering and x-ray rocking curves in the analyses of superlattices

A. H. Hamdi, V. S. Speriosu,* J. L. Tandon,[†] and M-A. Nicolet
California Institute of Technology, Pasadena, California 91125

(Received 17 September 1984)

Detailed compositional and structural analyses of superlattices have been carried out by mega-electron-volt He⁺ backscattering with channeling and with x-ray rocking curves. Through the combined use of the two techniques, depth profiles of strain, composition, and crystalline quality have been determined. An example of an Al_xGa_{1-x}As/GaAs strained-layer-superlattice (SLS) is considered. The thicknesses of the individual periods in these SLS structures were accurately measured by backscattering spectrometry. The values so obtained were used in the detailed calculations of x-ray rocking curves. Excellent agreement between measured and calculated curves was achieved. Transition regions at the interfaces of the various layers in the SLS were also detected and measured by both techniques. The two techniques complement each other and together provide powerful quantitative tools to characterize SLS structures.

I. INTRODUCTION

Modern epitaxial techniques, e.g., metal organic chemical vapor deposition (MOCVD) and molecular beam epitaxy, have made possible the growth of thin compound semiconductor superlattices. These structures, because of their unique optical and electrical properties,^{1,2} open up new possibilities in the fabrication of solid-state lasers and high-speed devices.³ Advancement in the realization of these devices demands a thorough characterization of the structure of the related materials. Analysis of such materials is also mandatory for the understanding of the physical phenomena associated with the performance of these devices.⁴ Material studies on strained-layer-superlattice (SLS) structures have been carried out by a variety of analytical techniques, e. g., Auger electron spectroscopy, secondary-ion mass spectrometry,⁵ transmission electron microscopy,⁶ x-ray diffraction,⁷ backscattering spectrometry (BS) with channeling,⁸⁻¹¹ etc.

In this paper, BS with channeling and x-ray rocking curves has been employed to analyze Al_xGa_{1-x}As/GaAs SLS structures. The combined use of the two techniques, along with the detailed interpretation of x-ray rocking curves, provides quantitative information on the depth distribution of strain, composition, and crystalline quality in the SLS structures. The power and complementary nature of these two techniques in analyzing SLS structures are demonstrated.

II. EXPERIMENTAL

The Al_xGa_{1-x}As/GaAs SLS samples were grown in a large-capacity MOCVD reactor on semi-insulating GaAs wafers oriented ~2° off the <100> axis.¹² Two structures, SLS1 and SLS2 with 10 and 15 periods, respectively, were grown. Each period consisted of two layers of Al_xGa_{1-x}As and GaAs. SLS1 had thinner layers than SLS2.

Backscattering spectrometry measurements were made with a 2.0-MeV He⁺ beam. In certain instances, to obtain

high depth resolution near the surface, the samples were tilted at an angle of 80° with respect to the beam. The detector had a resolution of ~ 18 keV. Channeling measurements were carried out along <100> and <110> axes. Adjustments in the tilt and azimuthal angles were made iteratively to obtain the lowest possible minimum yields. Angular scans of yield made around the angles so determined were symmetric. X-ray rocking-curve measurements were performed with a nearly monochromatic Fe K α_1 line. A computer-controlled double-crystal diffractometer was used. The beam was rendered nearly monochromatic by (400) reflection from a <100>-oriented GaAs crystal. The spot size of the x-ray beam was ~0.5×1.0 mm². Rocking curves were obtained from symmetric (200) and (400) reflections. The measured curves were fitted using a kinematic model of x-ray diffraction in thin epitaxial layers, while the diffraction in the substrate was treated dynamically.¹³

III. RESULTS

A. Backscattering spectrometry measurements

The capability of the BS technique in the analysis of SLS structures is illustrated in Fig. 1. Random spectra from the SLS2 and virgin GaAs samples are compared. Three distinct regions in the BS spectra in Fig. 1 can be identified. In region I, the oscillations in the SLS2 spectrum are due to the modulated concentration of Ga in the layers consisting of the SLS structures. The number of periods (=15) can clearly be counted. The SLS2 spectrum has a lower yield than the virgin GaAs spectrum in region I. This is because of a limited depth resolution of the system for a 25° tilted-angle geometry. Near the boundary of region II, the smearing of oscillations in region I can be explained by the interfering Al signal from the near-surface Al_xGa_{1-x}As layers. In the SLS2 spectrum, region II corresponds to the yield obtained from the GaAs substrate below the SLS structure. This yield is higher than the yield from the virgin GaAs sample be-

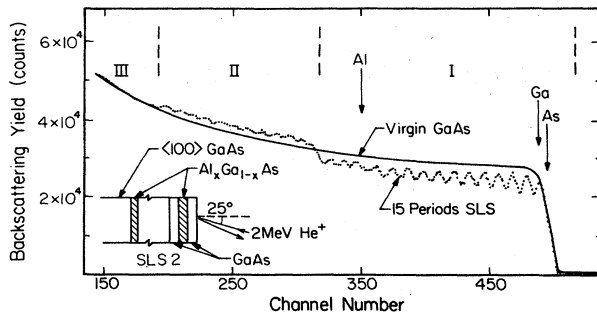


FIG. 1. BS spectra of 2-MeV He^+ obtained for random incidence on SLS2, 15 periods (dotted lines), and virgin GaAs samples (solid lines). The SLS spectrum contains 15 maxima and minima, in region I, which indicates the number of the $\text{Al}_x\text{Ga}_{1-x}\text{As}/\text{GaAs}$ periods.

cause of the added Al signals. The modulated Al signal from the SLS structure cannot be clearly detected in this region because of the high GaAs background level and the limited sensitivity of the BS technique to light elements in a heavy matrix (Al in GaAs in this case). BS yield from the SLS2 and the virgin GaAs samples are nearly identical in region III. This agreement is accidental, which may be due to the difference in charge collection during acquiring the two spectra. Calculations of the BS yield in region III using tabulated stopping cross-section and energy-loss values¹⁴ showed that the yield for the virgin GaAs should be $\sim 10\%$ higher than that for the SLS2 sample.

To analyze the surface layers of the SLS2 sample in further detail, a high-resolution BS spectrum was obtained with a tilted angle of 80° . This is shown in Fig. 2, along with the reference virgin GaAs spectrum. The BS yields from both the SLS2 and the virgin samples are identical at the surface, indicating the existence of a pure GaAs layer at the surface of SLS2. This result could not be ascertained from the spectrum in Fig. 1 because of limited resolution. The progressively lower yields of the GaAs layers below the surface of the SLS2 sample, when compared with the reference virgin GaAs sample (Fig. 2), are mainly due to the difference in the stopping powers of the He^+ beam in the two cases. In the high-resolution spectrum of the SLS2 sample, uneven transition regions at the interfaces of the GaAs and $\text{Al}_x\text{Ga}_{1-x}\text{As}$ layers can also be detected. Details of these regions with respect to their thicknesses and compositional variations will be discussed later.

Channeling measurements along $\langle 100 \rangle$ and $\langle 110 \rangle$ axes (not shown) were also carried out. The minimum yields of the SLS samples are similar to those of virgin GaAs, which confirms the high crystalline quality of the SLS structures. Angular scans made across the $\langle 110 \rangle$ axis with energy windows placed in the near-surface GaAs and $\text{Al}_x\text{Ga}_{1-x}\text{As}$ layers in both the SLS1 and SLS2 samples could not detect any strain in the superlattice structures. The precision of our channeling system is good enough to measure a strain of 1.2% in the ion-implanted materials.¹⁵ Thus in the $\text{Al}_x\text{Ga}_{1-x}\text{As}/\text{GaAs}$ SLS structures, the expected strain should be $< 1.2\%$.

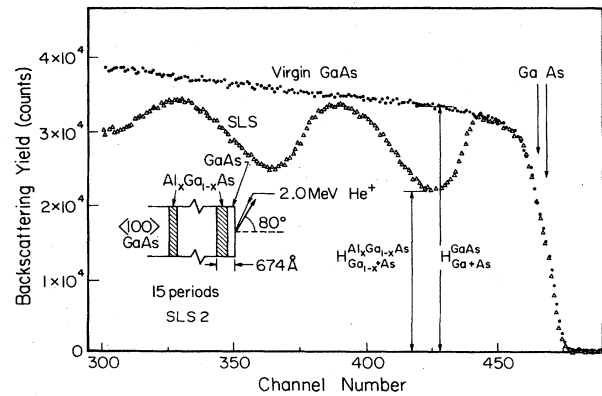


FIG. 2. High-resolution (80° tilted) BS spectra for random incidence on SLS2 and virgin GaAs samples. Near the surface, the yield from the SLS2 sample reaches the yield from the virgin GaAs sample, which implies that the surface layer in the SLS2 sample is pure GaAs.

B. X-ray rocking-curve measurements

X-ray rocking-curve measurements were made on both SLS1 and SLS2 samples. Figure 3(a) shows measurements made (dashed line) on the SLS1 sample with (200) reflection. The reflecting power plotted on the vertical axis has been normalized with respect to the power of the incoming beam. The angle $\Delta\theta$ is measured relative to the Bragg angle ($\theta_B \approx 20^\circ$). Several peaks (p_0, p_1, p_{-1}, \dots) in the rocking curve are due to the periodicity in the SLS structure. The substrate peak p_{sub} is embedded in the major SLS peak, p_0 in this case. In the kinematical regime, the reflecting power is proportional to the square of the structure factor.¹⁶ Since in the (200) reflection the structure factor of GaAs is an order of magnitude lower¹⁷ than that of $\text{Al}_x\text{Ga}_{1-x}\text{As}$, p_{sub} is buried in p_0 . Corresponding measurements were carried out in the (400) reflection, where p_{sub} and p_0 could be well separated. The average strain $\langle \epsilon \rangle$ in the SLS samples was measured from the (400) rocking curves (not shown), as follows:

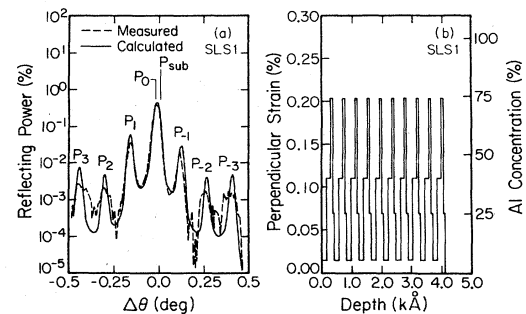


FIG. 3. (a) Plots of $\text{Fe } K\alpha_1$ (200) reflection x-ray rocking curves from sample SLS1. The dashed line is measured. The solid line is calculated by using the strain depth profile in (b).

$$\langle \epsilon \rangle = \frac{\epsilon_a t_a + \epsilon_b t_b}{t_a + t_b} = -\Delta\theta_0 \cot\theta_B, \quad (1)$$

where ϵ_a, ϵ_b and t_a, t_b are the strains and the thicknesses, respectively, of the two layers: a , $\text{Al}_x\text{Ga}_{1-x}\text{As}$ and b , GaAs , consisting of one period of the SLS sample: $\Delta\theta_0$ is equal to the angular difference between the peaks, p_0 and p_{sub} ; and θ_B is the Bragg angle of the substrate. Equation (1) is rigorously valid for perfectly periodic superlattice with two layers in each period.

The rocking curve measured in the (200) reflection provides a higher sensitivity to the thickness and composition variation in the periods of the SLS sample, when compared to the measurements in the (400) reflection.¹⁸ The (200) reflection case is thus considered here. Referring back to Fig. 3(a), the angular separations between subsidiary peaks ($\Delta\theta_{p_0-p_1}, \Delta\theta_{p_0-p_2}, \dots$) are all equal and are related, for symmetric reflections, to the average thickness of the period of the superlattice, according to the relation

$$\Delta\theta_p = \Delta\theta_{p_0-p_1} = \Delta\theta_{p_0-p_2} = \dots = \frac{\lambda}{2t \cos\theta_B}, \quad (2)$$

where λ is the wavelength of the x rays, and t is the average thickness of one period. The measured curve in Fig. 3 (a) (dashed line) was fitted with a calculated curve (solid line) using a kinematic model of x-ray diffraction in thin epitaxial layers. An iterative approach was adopted in the fitting, keeping the measured average strain [Eq. (1)] and the measured average thickness [Eq. (2)] values constant. Good fitting (note the logarithmic ordinate) was only obtained by accommodating transition regions at the interfaces of GaAs and $\text{Al}_x\text{Ga}_{1-x}\text{As}$ layers. The average depth strain profile for this fitting is shown in Fig. 3(b). The Al concentration is also plotted in Fig. 3(b), since by Vegard's law,¹⁹ perpendicular strain is linearly proportional to the Al concentration in the $\text{Al}_x\text{Ga}_{1-x}\text{As}$ layers. Another important inference from Fig. 3(b) is that in the growth of the SLS1 sample, pure GaAs layers were not achieved.

IV. DISCUSSION

Figures 1 through 3 provide insight into the structural properties of $\text{Al}_x\text{Ga}_{1-x}\text{As}/\text{GaAs}$ SLS samples. In particular, the combined use of the two techniques (BS and x-ray rocking curves) gives information on the depth distribution of strain, composition, and crystalline quality. In this section, we demonstrate the complementary aspects of the two techniques in providing further details.

A. Individual period thickness determination

The ability of BS to determine the thicknesses of multilayered thin films is well established.¹⁴ The thicknesses of the periods of the SLS1 and SLS2 samples were determined from the stopping-power data¹⁴ of He^+ in GaAs and $\text{Al}_x\text{Ga}_{1-x}\text{As}$ layers. For these calculations, the nom-

inal value of $x=0.88$ in the $\text{Al}_x\text{Ga}_{1-x}\text{As}$ layers was assumed as estimated from growth parameters. This value of x was later verified by BS and x-ray measurements (see Figs. 2 and 3). For individual period-thickness calculations, the energy loss between the two adjacent peaks in the BS spectrum (see Fig. 1) was used. The average period thickness was also estimated by dividing the total thicknesses of the SLS samples by their respective number of periods. For the total-thickness calculations, the energy loss between regions I and II in Fig. 1 was used. The individual period thicknesses in SLS1 and SLS2 samples are plotted in Fig. 4, along with the average period thicknesses. The average thickness measurements made by BS agreed very well with those obtained by the x-ray rocking curves. Variation in the individual period thicknesses of the SLS samples are noticeable from Fig. 4, which may be related to the growth parameters. The relatively strong deviation from the average period thickness near the substrate interface may be due to the uncertainty in estimating the peaks in SLS BS spectra (see Fig. 1) due to the interfering Al signals.

The individual period thicknesses obtained by BS measurements, as described above, were then used to recalculate the x-ray rocking curve of the SLS1 sample. In this calculation, the parameters used were similar to those in Fig. 3(b), except that the thicknesses of the individual periods were now varied according to the BS results of Fig. 4, while keeping the sum of the products of strains and thicknesses in each period constant [see Eq. (1)]. The calculated rocking curve so obtained is compared with the measured curve in Fig. 5(a). The corresponding depth strain profile is shown in Fig. 5(b). As can be observed, better agreement between calculated and measured curves is achieved in Fig. 5(a) when compared with Fig. 3(a), especially for higher-order peaks. Notice here that BS and x-ray rocking-curve techniques provide details on the structure of the SLS samples that nicely complement each other. The variation in the period thicknesses of the SLS samples can thus be claimed as real with good confidence.

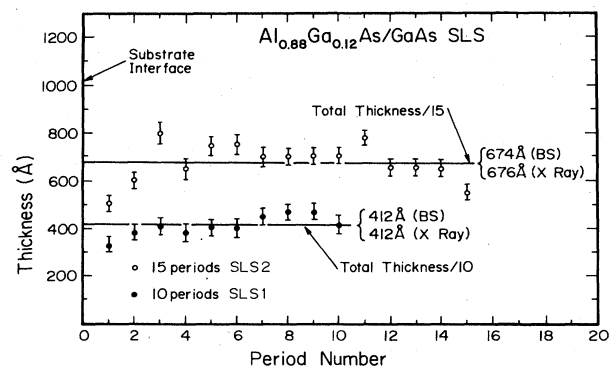


FIG. 4. The individual and average period thicknesses of SLS1 (10 periods) and SLS2 (15 periods) derived from BS spectra as shown in Fig. 1 for the SLS2 sample. X-ray thicknesses were extracted from the fitted rocking curves in (200) and (400) reflections, e. g., as shown in Fig. 3 for the SLS2 sample.

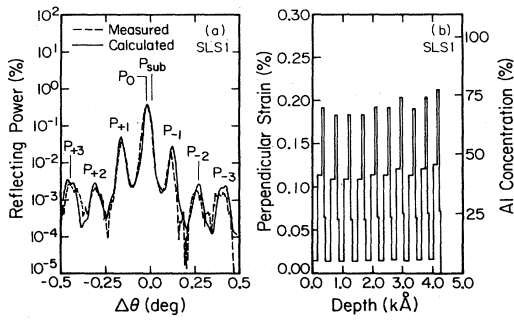


FIG. 5. (a) The dashed line is the $\text{Fe } K\alpha_1$ rocking curve for the (200) reflection measured from the SLS1 sample shown also in Fig. 3(a). The solid-line rocking curve was calculated by using the thickness of the individual periods measured by BS (Fig. 4) which gave the depth profile of strain shown in (b).

B. Transition regions

In the analyses of the SLS1 and SLS2 samples, the transition regions between the $\text{Al}_x\text{Ga}_{1-x}\text{As}$ and GaAs sublayers are detected by both BS and x-ray rocking curves (see Figs. 2 and 3). The aluminum concentration and strain profile as a function of depth in the first period below the surface of the SLS2 sample is shown in Fig. 6. The profile derived from x-ray rocking curves was obtained in a fashion as is described in Fig. 3(b). The steps in this profile are merely representative of the real distribution, which should be continuous.²⁰ The Al-concentration profile, measured by BS and plotted in Fig. 6, was obtained from Fig. 2. The Al concentration (x) was calculated from the heights $H_{\text{Ga}_{1-x}\text{As}}^{\text{Al}_x\text{Ga}_{1-x}\text{As}}$ and $H_{\text{Ga+As}}^{\text{GaAs}}$ as defined in Fig. 2, using the relation

$$\frac{H_{\text{Ga+As}}^{\text{GaAs}}}{H_{\text{Ga}_{1-x}\text{As}}^{\text{Al}_x\text{Ga}_{1-x}\text{As}}} = \frac{\gamma_{\text{Ga}} + \gamma_{\text{As}}}{(1-x)\gamma'_{\text{Ga}} + \gamma'_{\text{As}}}, \quad (3)$$

where $H_{\text{Ga+As}}^{\text{GaAs}}$ and $H_{\text{Ga}_{1-x}\text{As}}^{\text{Al}_x\text{Ga}_{1-x}\text{As}}$ are the total BS yields from Ga and As in pure GaAs and $\text{Al}_x\text{Ga}_{1-x}\text{As}$, respectively. γ_{Ga} , γ_{As} , γ'_{Ga} , γ'_{As} are the ratios of the scattering to the stopping cross section parameters of He^+ from Ga and As in GaAs and in $\text{Al}_x\text{Ga}_{1-x}\text{As}$, respectively.¹⁴ The accuracy in the composition measurement is within $\pm 1\%$. Excellent agreement in the transition regions as determined by BS and x-ray curves is observed. The complementary nature of the two techniques is again exempli-

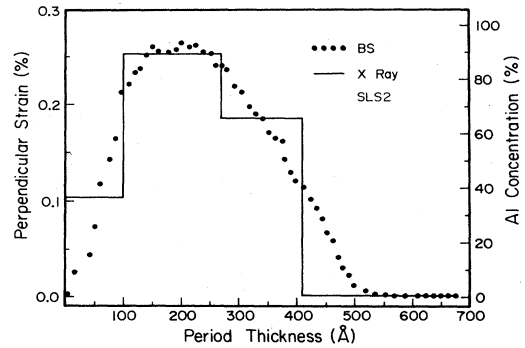


FIG. 6. Depth distribution of strain and the Al concentration in the first period of the SLS2 sample. The strain profile was derived from the x-ray rocking curve, as explained in Fig. 3. The Al concentration profile was determined from the BS spectrum of Fig. 2 (see text). Excellent agreement exists between the two techniques.

fied. The nonsymmetric and nonabrupt profile within a period of the SLS is real and related to the growth process.²⁰

V. CONCLUSIONS

The combined use and power of BS and x-ray rocking curves in analyzing $\text{Al}_x\text{Ga}_{1-x}\text{As}/\text{GaAs}$ SLS structures have been demonstrated. The two techniques complement each other in providing detailed information on the depth distribution of strain, composition, and crystalline quality in these structures. Such detailed information has not been accessible by previously used techniques. The analyses carried out in this paper can be easily extended to a variety of other strained-layer-superlattice structures. The quantitative information thus obtained should prove useful not only to the growers of SLS, but also in exploring their future uses in device structures.

ACKNOWLEDGMENTS

We would like to thank Y. C. M. Yeh, D. A. Smith, A. Mehta, and J. Wendt at Applied Solar Energy Corporation (ASEC) for the growth of SLS structures. Encouragement provided by K. S. Ling and P. A. Iles at ASEC is appreciated. A. H. Hamdi extends his thanks to IBM for financial support. The work was supported by the Defense Advanced Research Projects Agency under Contract No. MDA 903-82-C-0348 at Caltech.

*Present address: IBM Research Laboratories, 5600 Cottle Road, San Jose, California 95193.

†Permanent address: Applied Solar Energy Corporation, City of Industry, California 91749.

¹J. N. Schulman and T. C. McGill, Phys. Rev. B 23, 4149 (1981).

²L. Esaki and L. L. Chang, Phys. Rev. Lett. 33, 495 (1974).

³W. D. Laidig, N. Holonyak, Jr., M. D. Camras, K. Hess, J. J.

Coleman, P. D. Dapkus, and J. Bardeen, Appl. Phys. Lett. 38, 776 (1981).

⁴G. C. Osbourn, J. Appl. Phys. 53, 1586 (1982).

⁵J. W. Lee and W. D. Laidig, J. Electron. Mater. 13, 147 (1984).

⁶C. M. Serrano and Chin-An Chang, Appl. Phys. Lett. 39, 808 (1981).

⁷A. Segmüller, P. Krishna, and L. Esaki, J. Appl. Crystallogr. 10, 1 (1977).

- ⁸W. K. Chu, F. W. Saris, C.-A. Chang, R. Ludeke, and L. Esaki, *Phys. Rev. B* **26**, 1999 (1982).
- ⁹S. T. Picraux, L. R. Dawson, G. C. Osbourn, R. M. Biefield, and W. K. Chu, *Appl. Phys. Lett.* **43**, 1020 (1983).
- ¹⁰W. K. Chu, C. K. Pan, and C.-A. Chang, *Phys. Rev. B* **28**, 4033 (1983).
- ¹¹W. K. Chu, T. A. Ellison, S. T. Picraux, R. M. Biefield, and G. C. Osbourn, *Phys. Rev. Lett.* **52**, 125 (1984).
- ¹²J. L. Tandon and Y. C. M. Yeh, *J. Electrochem. Soc.* (to be published).
- ¹³V. S. Speriosu, *J. Appl. Phys.* **52**, 6094 (1981).
- ¹⁴W. K. Chu, J. W. Mayer, and M.-A. Nicolet, *Backscattering Spectrometry* (Academic, New York, 1978).
- ¹⁵B. M. Paine, V. S. Speriosu, L. S. Wieluński, H. L. Glass, and M.-A. Nicolet, *Nucl. Instrum. Methods* **191**, 80 (1981).
- ¹⁶W. H. Zachariasen, *Theory of X-Ray Diffraction in Crystals* (Wiley, New York, 1945).
- ¹⁷The structure factors of $\text{Al}_{0.88}\text{Ga}_{0.12}\text{As}$ ($=61.1$) and GaAs ($=6.4$) were calculated from tables of atomic scattering factors for x rays; J. A. Ibers and W. C. Hamilton, *International Tables for X-Ray Crystallography* (Kymoch, Birmingham, 1974), Vol. IV.
- ¹⁸V. S. Speriosu and T. Vreeland, Jr., *J. Appl. Phys.* **56**, 1591 (1984).
- ¹⁹W. J. Bartels and W. Nigman, *J. Cryst. Growth* **44**, 518 (1978).
- ²⁰A. H. Hamdi, V. S. Speriosu, M.-A. Nicolet, J. L. Tandon, and Y.C.M. Yeh, *J. Appl. Phys.* **57**, 1400 (1985).